THE JOURNAL OF BIOLOGICAL CHEMISTRY VOL. 289, NO. 46, pp. 31662–31672, November 14, 2014
Published in the U.S.A.

Transformer 2β homolog (*Drosophila*) (TRA2B) Regulates Protein Kinase C δI (PKCδI) Splice Variant Expression during 3T3L1 Preadipocyte Cell Cycle*

Received for publication, June 30, 2014, and in revised form, September 23, 2014 Published, JBC Papers in Press, September 26, 2014, DOI 10.1074/jbc.M114.592337

Rekha S. Patel[‡1], **Gay Carter**[§1], **Denise R. Cooper**[‡§], **Hercules Apostolatos**[‡], **and Niketa A. Patel**[‡§2]
From the [§]*James A. Haley Veterans Hospital and* [‡]*Department of Molecular Medicine, University of South Florida, Tampa, Florida 33612*

Background: PKCδ modulates cellular differentiation and proliferation.
Results: Splice factor TRA2B regulates alternative splicing of PKCδI.
Conclusion: PKCδI is a gate-keeper of adipocyte differentiation.
Significance: Understanding the role and regulation of PKCδI during adipogenesis may contribute toward developing a novel target for managing obesity and its co-morbidities.

Obesity is characterized by adipocyte hyperplasia and hypertrophy. We previously showed that PKCδ expression is dysregulated in obesity (Carter, G., Apostolatos, A., Patel, R., Mathur, A., Cooper, D., Murr, M., and Patel, N. A. (2013) *ISRN Obes.* 2013, 161345). Using 3T3L1 preadipocytes, we studied adipogenesis *in vitro* and showed that expression of PKCδ splice variants, PKCδI and PKCδII, have different expression patterns during adipogenesis (Patel, R., Apostolatos, A., Carter, G., Ajmo, J., Gali, M., Cooper, D. R., You, M., Bisht, K. S., and Patel, N. A. (2013) *J. Biol. Chem.* 288, 26834–26846). Here, we evaluated the role of PKCδI splice variant during adipogenesis. Our results indicate that PKCδI expression level is high in preadipocytes and decreasing PKCδI accelerated terminal differentiation. Our results indicate that PKCδI is required for mitotic clonal expansion of preadipocytes. We next evaluated the splice factor regulating the expression of PKCδI during 3T3L1 adipogenesis. Our results show TRA2B increased PKCδI expression. To investigate the molecular mechanism, we cloned a heterologous splicing PKCδ minigene and showed that inclusion of PKCδ exon 9 is increased by TRA2B. Using mutagenesis and a RNA-immunoprecipitation assay, we evaluated the binding of Tra2β on PKCδI exon 9 and show that its association is required for PKCδI splicing. These results provide a better understanding of the role of PKCδI in adipogenesis. Determination of this molecular mechanism of alternative splicing presents a novel therapeutic target in the management of obesity and its co-morbidities.

Adipose tissue in the body is composed mainly of fat cells (adipocytes). Adipogenesis is a process in which preadipocytes differentiate into adipocytes. The study of adipogenesis, including the underlying cellular processes and molecular mechanisms, is important to understanding obesity. A widely used *in vitro* model to study adipogenesis is the 3T3L1 cell line, which was established by Green and Kehinde (3, 4). It authentically reproduces adipogenesis including expression of adipogenic genes and morphological changes. Confluent preadipocytes upon treatment with differentiation mixture enter differentiation (day 0). Cells undergo mitotic clonal expansion during which they re-enter the cell cycle, and by day 4 they are terminally differentiated. Mature adipocytes are usually established by day 7 in culture. Adipogenesis is regulated transcriptionally by PPARγ[3] and C/EBP family and their co-factors, which promote the morphological and functional changes of a preadipocyte to an adipocyte phenotype characterized by cell shape and lipid accumulations (5–7).

Protein kinase Cδ (PKCδ) is a member of the serine threonine PKC family. The PKC family consists of 11 isoforms and their splice variants and is involved in the regulation of cellular differentiation, growth, and apoptosis (8). The expression of PKCδ splice variants is species-specific. PKCδI is ubiquitously present in all species. We have demonstrated the function of PKCδI in promoting apoptosis and PKCδII and PKCδVIII as pro-survival proteins (9, 10). The functions of other PKCδ splice variants are not yet established.

Alternative pre-mRNA splicing generates genetic diversity. This post-transcriptional process results in the expression of multiple proteins from a single gene. Alternative splicing is known to occur in >85% of genes. Trans-factors interact with pre-mRNA cis-elements to regulate alternative splicing. Splicing trans-factor SFRS10 (also known as TRA2B/Tra2β) belongs to a large family of serine-arginine (SR)-rich proteins. These proteins bind to the pre-mRNA to promote splicing of an exon. During development, alternative splicing is often regulated by the levels of the splicing trans-factors.

* This work was supported by a Department of Veterans Affairs Medical Research Grant 821-MR-EN-20606 (to N. A. P.).
[1] Both authors contributed equally to this work.
[2] To whom correspondence should be addressed: James A. Haley Veterans Hospital, Research Service VAR 151, 13000 Bruce B. Downs Blvd., Tampa, FL 33612. Tel.: 813-972-2000 (ext. 7283); Fax: 813-972-7623; E-mail: Niketa.Patel@va.gov; npatel@health.usf.edu.

[3] The abbreviations used are: PPAR, peroxisome proliferator-activated receptor; C/EBP, CCAAT-enhancer-binding protein; TRA2B, transformer 2 β homolog (*Drosophila*); RIP, RNA immunoprecipitation; SD, splice donor; SA, splice acceptor; qPCR, quantitative PCR; IP, immunoprecipitation; PRKCD, protein kinase Cδ.

TRA2B (transformer 2β homolog (*Drosophila*)) is also known as SFRS10 (11). It is highly conserved across human, mouse, and flies. A new nomenclature was introduced by Manley and Krainer (12) for SR proteins in 2010. According to this nomenclature, members of the SR family of splicing factors are numbered according to the chronological order of their discovery. Based on this they have assigned SRSF10 (SR splicing factor 10) name to the splicing factor TASR1/SRp38/SRrp40. This nomenclature is not to be confused with TRA2B/SFRS10 splicing factor discussed here. Mammalian Tra2 has two isoforms: Traα and Tra2β. Tra2α plays a role in sexual differentiation similar to that in *Drosophila* (13). TRA2B is alternatively spliced to TRA2B1, -2, -3, -4, and -5. TRA2B1 mRNA generates a full-length protein, whereas TRA2B2 through -B5 generate truncated proteins lacking parts of RS (arginine/serine repeats) domain whose function *in vivo* has not yet been established. The role of TRA2B in alternative splicing is attributed to TRA2B1 (14). TRA2B has two RS domains flanking the central RNA recognition motif domain. TRA2B autoregulates its protein expression (15).

Here, we evaluated adipogenesis and the role of PKCδI during early phases of differentiation of 3T3L1 preadipocytes. Furthermore, we identified the splice factor mediating the expression of PKCδI splice variant in 3T3L1 cells.

EXPERIMENTAL PROCEDURES

Cell Culture—Mouse 3T3-L1 preadipocytes were purchased from ATCC® CL-173™ and passaged as preconfluent cultures in Dulbecco's modification of Eagle's medium (DMEM) high glucose (Invitrogen) with 10% newborn calf serum (Sigma) at 37 °C and 10% CO_2. Once confluent (day 0), cells were differentiated in DMEM high glucose with 10% fetal bovine serum (Atlas Biological, Fort Collins, CO), 10 μg/ml bovine insulin (Sigma), 1 mM dexamethasone (Sigma), and 0.5 mM isobutyl-1-methylxanthine (Sigma). On day 2, media were replaced with DMEM high glucose, 10% FBS, and bovine insulin. Day 4 and onward, cells were cultured in DMEM high glucose plus 10% FBS.

Flow Cytometry—Cells were trypsinized and washed one time with phosphate-buffered saline (PBS). The cell pellet (containing one million cells) was resuspended in 500 μl of PBS and fixed by the slow, dropwise addition of 4.5 ml of ice-cold 70% ethanol while vortexing. Samples were incubated overnight at 4 °C to complete fixation and then stored at −20 °C until stained. Fixed cells were centrifuged at 1000 rpm for 5.0 min. The cell pellet was washed twice with PBS. The cell pellet was resuspended in 50 μl of RNase A (100 μg/ml) and incubated at room temperature for 5.0 min. One ml of PBS was added, and samples were divided to create an unstained negative control for cell cycle analysis. Propidium iodide (50 μg/ml in PBS) was added to samples to be stained and samples were incubated at 37 °C for 30 min and then analyzed on the Accuri C6 flow cytometer using the FL2 channel. Pulse analysis was used to gate the single cell population and then scatter plot gating was applied to remove debris. Markers were set based on the propidium iodide histogram, and the percentage of G_0G_1, S phase, and G_2/M cells was calculated by the Accuri C6 software.

Western Blot Analysis—Protein lysates were obtained from 3T3L1 cells using lysis buffer containing protease inhibitors. Protein lysates (40 μg) were separated by SDS-PAGE on 10% gels. Proteins were electrophoretically transferred to nitrocellulose membranes, blocked with Tris-buffered saline containing 0.1% Tween 20 and 5% nonfat dried milk, washed, and incubated with anti-PKCδ (Cell Signaling), PKCδII-specific antibody (16), anti-Tra2β (Sigma), anti-PPARγ (Santa Cruz Biotechnology), anti-PGC1α (Santa Cruz Biotechnology), and β-actin A5441 (Sigma). After incubation with anti-rabbit IgG-HRP, enhanced chemiluminescence (Pierce) was used for detection. The FluorChem M™ (Protein Simple) imaging system was used to capture digital chemiluminescence images and processing Western blots. Data were analyzed using AlphaView® software.

PCR—Total RNA was isolated from 3T3L1 cells with RNA-Bee (Tel Test Inc.) as recommended by the manufacturer. Two μg of RNA was used to synthesize first-strand cDNA with oligo(dT) primer or random hexamer primer and the Omniscript R kit (Qiagen). The following primers were used in PCR for the splicing minigene: PKCδ forward primer 5′-CATCCTAGGTCCTGCGACAA-3′; β-actin forward primer 5′-CTTCATTGACCTCAACTCATG-3′; reverse primer 5′-TGTCATGGATGACCTTGGCCAG-3′; SD primer 5′-TCTGAGTCACCTGGACAACC-3′; SA primer 5′-ATCTCAGTGGTATTTGTGAGC-3′. After PCR, 5% of products were resolved on 6% PAGE gels and detected by silver staining. The PCR reaction was optimized for linear range amplification to allow for quantification of products. Data were analyzed using AlphaView® software.

Quantitative Real-time qPCR—Total RNA was isolated from 3T3L1 cells using RNAzol according to the manufacturer's protocol (TelTest Inc.). Two μg of RNA were reverse-transcribed with an Omniscript R kit (Qiagen) using oligo(dT) primers or random hexamer primers (for the RNA-immunoprecipitation (RIP) assay). QPCR was performed using 1.0 μl of cDNA and Maxima SYBR Green/Rox qPCR master mix (Thermo Scientific). The primers used were: PKCδI sense primer 5′-ACATCCTAGACAACAACGGGAC-3′ and antisense 5′ ACCACGTCCTTCTTCAGACAC-3′; PKCδII sense primer 5′-CACCATCTTCCAGAAAGAACG-3′ and antisense 5′TCGCAGGTCTCACTACTGCCTTTTCC-3′; GAPDH sense primer 5′-TGACGTGCCGCCTGGAGAAAC-3′ and antisense 5′-CCGGCATCGAAGGTGGAAGAG-3′. Amplification was performed on the ViiaA 7 (Applied Biosystems). Real-time PCR was then performed in triplicate on samples and standards. The plate setup included a standard series, no template control, no RNA control, no reverse transcriptase control, and no amplification control. After primer concentrations were optimized to give the desired standard curve and a single melt curve, relative quotient was determined using the $\Delta\Delta C_T$ method with GAPDH as the endogenous control and day 0 as the calibrator sample. Experiments were repeated four times.

siRNA Transfection—PRKCD siRNA (ID: 103702), PKCδII-specific siRNA (ID: 444054), and scrambled siRNA were purchased from Ambion. TRA2B siRNA (ID: SR408282 A, B, C) and its scrambled control were purchased from Origene. In our experiments SR408282 A gave optimal results. These siRNA were previously validated for specificity, and off-target gene effects were eliminated. The siRNAs were transfected for

48–72 h using siPORT NeoFX® transfection agent or siTRAN transfection agent.

Transient Transfection of Plasmid DNA—3T3L1 preadipocytes were trypsinized, and cell pellets were collected in 100 μl of Nucleofector® solution (Lonza) and combined with plasmid DNA (2 μg). The cell/DNA solution was transferred to a cuvette, and the program was initiated (0.34kV, 960 microfarads). Medium (500 μl) was added immediately, and cells were gently transferred to 60-mm plates and allowed to differentiate. In some experiments Trans-IT 3T3™ (Mirus Bio LLC) transfection agent was used according to the manufacturer's instructions.

Oil Red O Staining—3T3L1 preadipocytes were washed with PBS and fixed with 10% formalin for 30 min. The cells were then rinsed and incubated with Oil Red O staining solution (Adipogenesis Assay kit, Millipore) and incubated for 15 min. After washing, images were captured with Nikon confocal microscope. For quantification, 250 μl of dye extraction solution was added and incubated for 30 min. Absorbance was read at 520 nm.

Construction of pSPL3-PKCδ Minigene—The pSPL3 vector was modified to remove cryptic 5′ splice sites as described in our previous publication (10). The pSPL3 vector was digested with BamHI (in the MCS) and NheI. Primers to amplify genomic PKCδ from 3T3L1 cells flanked mouse PKCδ exon 9 (101 bp) and were designed to include the BclI site in the forward primer (in bold type below) and BcuI site in the reverse primers (in bold type). The forward primer was designed to amplify 49 bp of 3′ intronic sequence such that the product contained the branch point and 3′ splice site and the reverse primer included 123 bp of 5′ intronic sequence (splicing minigene A) or 34 bp of 5′ intronic sequence (minigene B). The primers were: forward primer 5′-TGG**TGATCA**AGGAATGAGACCTGGGAGACC-3′; reverse primer Minigene A 5′-AGA**ACTAGT**TTTCAGTCTACATGACTCCC-3′; reverse primer Minigene B 5′-GATA**CTAGT**AAAGAGATATGTGACCCAGC-3′. The products were verified by sequencing and ligated into the digested pSPL3 vector. The overhangs of the selected restriction enzymes hybridized, and this enabled cloning of the PCR product in the proper orientation. The resulting splicing minigenes were verified by restriction digestion and sequencing.

Mutation of Minigene—Mutation was created at the TRA2B site on the splicing minigene A using the QuikChange II site-directed mutagenesis kit (Agilent Technologies # 200523-5) according to the manufacturer's instructions. The primers used to create the mutation were 5′-GGAATATACCAGGGATTTGAGCCTAAGCCAGAAGTCTCTGGGAGT-3′ (sense) and 5′-ACTCCCAGAGACTTCTGGCTTAGGCTCAAATCCCTGGTATATTCC-3′ (antisense). Mutation to the plasmid was confirmed by DNA sequencing. The mutated minigene is referred to as pSPL3-PKCδ**T2b minigene.

RIP Assay—The RIP kit was purchased from Sigma, and the protocol was followed as per the manufacturer's instruction. Tra2β antibody was purchased from Sigma, SNRNP70 antibody was from Millipore, and IgG antibody was included in kit (Sigma). Cell lysate (10%) was removed for the input sample. Immunoprecipitation was performed with 2 μg of Tra2β antibody, SNRNP70 antibody (positive control), or IgG antibody (as the negative control). RNA was purified and treated with DNase to remove genomic DNA. SYBR Green real-time qPCR was performed as described above using PKCδ primer sets and primers for U1 RNA, the binding partner for the positive control SNRNP70. The primer sequences for U1 RNA are: forward 5′-TCCCAGGGCGAGGCTTATCCATT-3′ and reverse 5′-GAACGCAGTCCCCCACTACCACAAAT-3′. The yield (% input) and specificity (-fold enrichment) was calculated using Excel™ template for RIP from Sigma.

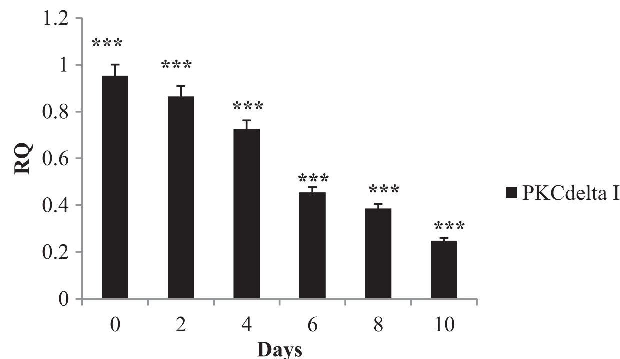

FIGURE 1. **3T3L1 preadipocytes were differentiated *in vitro* and RNA was isolated every 2 days from day 0 to day 10.** Real-time qPCR was performed in triplicate using PKCδI-specific primers and GAPDH as the internal control. The graph shows relative quantification (*RQ*) for PKCδI over 0–10 days. The experiment was independently repeated five times with similar results. Statistical analysis performed by two-way analysis of variance; ***, $p < 0.0001$ highly significant within the group.

Statistical Analysis—The PCR gels for the splicing minigene assay and the Western blots were analyzed using AlphaView® software from ProteinSimple™. Experiments were repeated three to five times for reproducibility. PRISM™ software was used for statistical analysis. Two-way analysis of variance or matched Student's *t* test was used in the analysis. A level of $p <$ 0.05 was considered statistically significant.

RESULTS

Expression Pattern of PKCδI during in Vitro Differentiation of 3T3L1 Preadipocytes—We previously showed that expression levels of PKCδ splice variants PKCδI and PKCδII switched by day 4 of differentiation (2). Here we sought to evaluate the role of PKCδI during adipogenesis. Using primers specific to PKCδI, our real time qPCR results (Fig. 1) indicate that PKCδI levels were high in preadipocytes and started declining after day 4 when the cells underwent terminal differentiation.

PKCδI Regulates Cell Cycle in 3T3L1 Cells—Our results indicated that PKCδI levels were higher during 3T3L1 preadipocyte mitotic clonal expansion (0–48 h upon hormonal induction). To determine its role in cell cycle, we knocked down the expression using PRKCD siRNA (25 nM; transfected on day −1 or scrambled siRNA (25 nM), and cells were harvested 0–24 h of differentiation). Using SYBR Green real time qPCR, we showed PRKCD siRNA decreased PKCδI levels, whereas PKCδII levels remained unaffected. Using flow cytometry, we determined the percentage of cells in the G_0/G_1, S, and G_2/M phase in 3T3L1 control (untreated), scrambled siRNA control, and PRKCD siRNA-transfected cells. Our results indicated that PRKCD siRNA decreased the percentage of cells in the G_2M phase (Fig. 2). The cells transfected with scrambled siRNA did not differ significantly from the control (untreated) cells indicating that

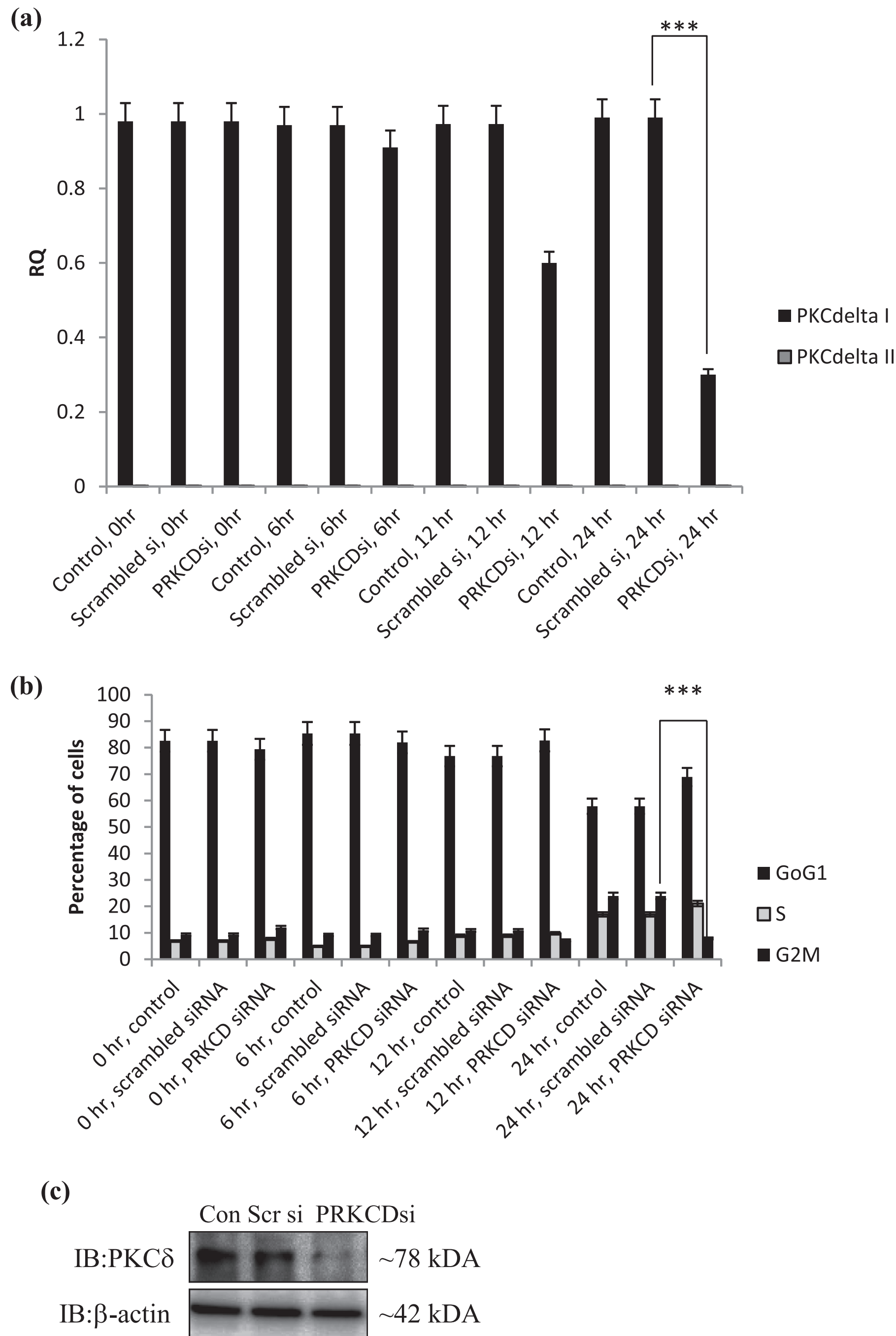

FIGURE 2. **PRKCD siRNA or scrambled siRNA was transfected on day −1 in 3T3L1 cells and maintained in culture with differentiation media.** Cells were harvested at 0, 6, 12, or 24 h and analyzed. *a*, SYBR Green real time qPCR using primers specific for PKCδI or PKCδII. qPCR results indicate decreased PKCδI at significant levels at 24 h (day 1 of differentiation). PKCδII expression was very low in this time period and was not affected by PRKCD siRNA. *RQ*, relative quantification. *b*, cell cycle analysis at 0, 6, 12, and 24 h of initiation of differentiation. Cell cycle analysis was performed with propidium iodide staining in flow cytometry, and the graph represents the percentage of cells in either G_0G_1, S, or G_2M phase at the indicated times. Experiments were repeated four times with similar results. Statistical analysis was performed by two-way analysis of variance; ***, $p < 0.0001$ highly significant between 24 h scrambled (*Scr*) siRNA control (*Con*) and PRKCD siRNA. *c*, Western blot (*IB*) analysis of the above samples at 24 h using anti-PKCδ antibody or β-actin. PRKCD siRNA decreased PKCδI; PKCδII (expected at 80 kDa) was not detected at 24 h. The experiment was repeated three times with similar results.

transfection of siRNA did not affect differentiation. This indicated an exit of the cell cycle with knockdown of PKCδI.

PKCδI Is an Inhibitor of Adipocyte Differentiation—Because our results indicated a role of PKCδI in preadipocyte differentiation, we transfected PRKCD siRNA along with its scrambled control as described above. Cells were differentiated to day 3. Formation of lipid droplets was evaluated with Oil Red O staining. Images were taken using a Nikon microscope, and the amount of Oil Red O staining was also quantified (see "Experimental Procedures"). Our results (Fig. 3, *a* and *b*) indicated that knockdown of PRKCD increased Oil Red O staining compared with control cells, indicating an increase in differentiation in the PRKCD siRNA cells. The cells transfected with scrambled siRNA did not differ significantly from the control (untreated)

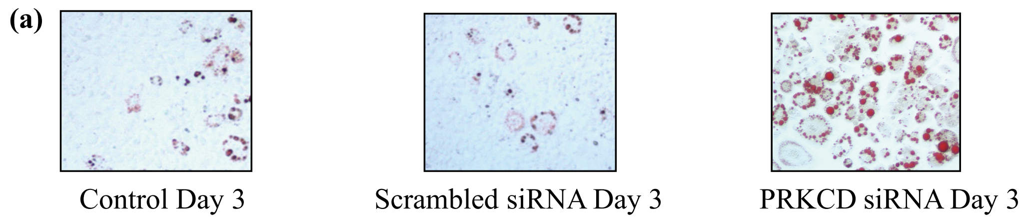
(a)
Control Day 3
Scrambled siRNA Day 3
PRKCD siRNA Day 3

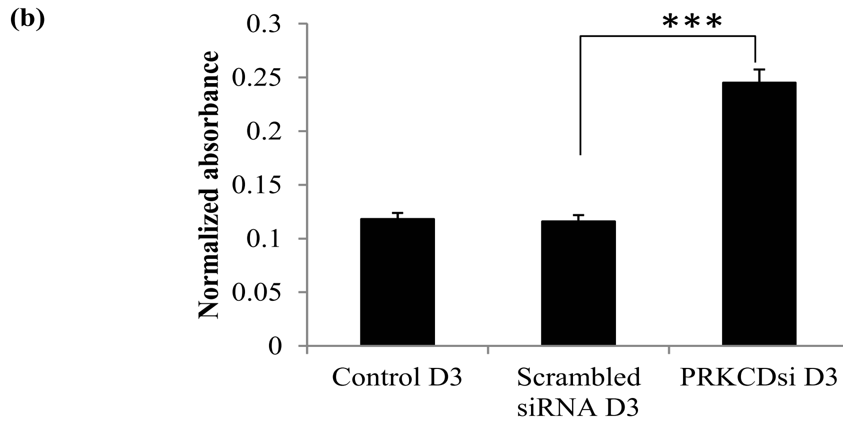
(b)
***
Normalized absorbance
0.3
0.25
0.2
0.15
0.1
0.05
0
Control D3
Scrambled siRNA D3
PRKCDsi D3

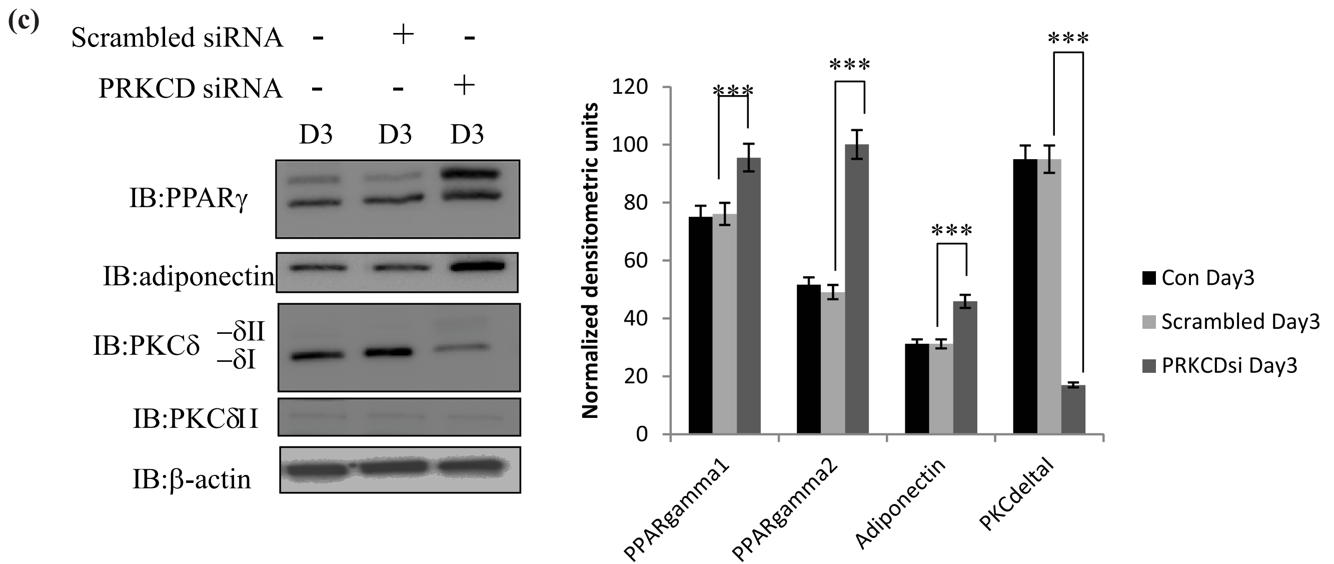
(c)
Scrambled siRNA - + -
PRKCD siRNA - - +
D3 D3 D3
IB:PPARγ
IB:adiponectin
IB:PKCδ –δII –δI
IB:PKCδII
IB:β-actin
Normalized densitometric units
120
100
80
60
40
20
0
***
PPARgamma1
PPARgamma2
Adiponectin
PKCdeltaI
Con Day3
Scrambled Day3
PRKCDsi Day3

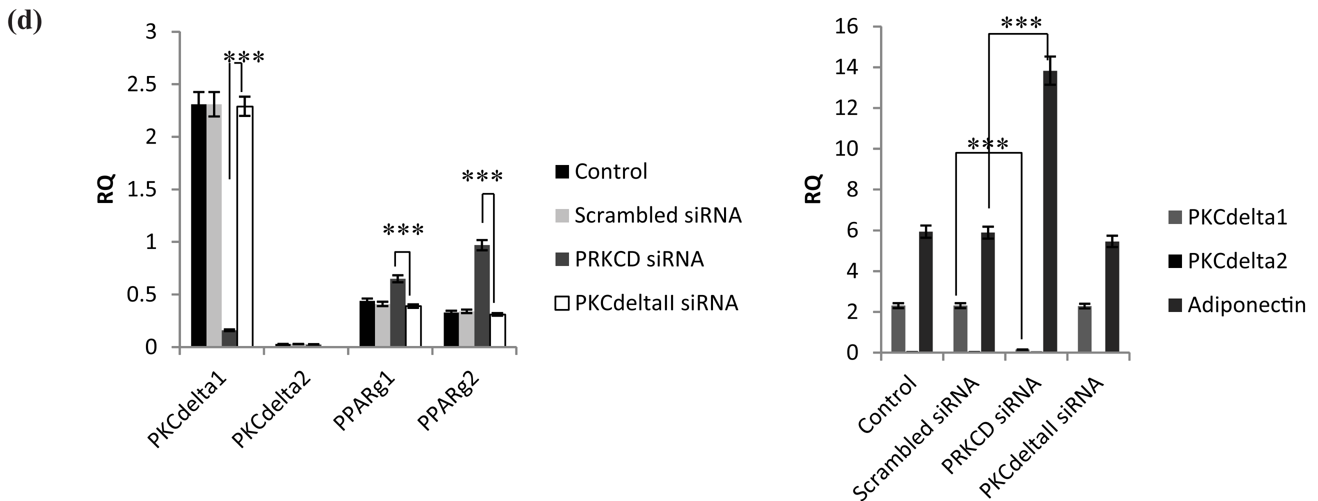
(d)
RQ
3
2.5
2
1.5
1
0.5
0
***
PKCdelta1
PKCdelta2
PPARg1
PPARg2
Control
Scrambled siRNA
PRKCD siRNA
PKCdeltaII siRNA
16
14
12
10
8
6
4
2
0
Control
Scrambled siRNA
PRKCD siRNA
PKCdeltaII siRNA
PKCdelta1
PKCdelta2
Adiponectin

cells. To validate that a decrease in PKCδI levels promoted adipocyte differentiation, we analyzed PPARγ and adiponectin, the markers for adipocyte differentiation, in cells transfected with PRKCD siRNA as described above. Using Western blot analysis (Fig. 3*c*), our results indicated an increase in PPARγ1 and -2 and adiponectin along with a decrease in PKCδI levels. PKCδII levels were not affected by PRKCD siRNA. Although PKCδII is not significantly expressed during early differentiation process (0 to 72 h), as a control we transfected either PKCδII siRNA or PRKCD siRNA on day 0, and cells were analyzed by SYBR Green real time qPCR on day 3 as shown (Fig. 3*d*). Results showed no significant changes in PPARγ1/2 with PKCδII siRNA, whereas PRKCD siRNA results were in agreement with the protein levels. These results suggest that inhibition of PKCδI allowed the cells to exit the cell cycle and initiate terminal differentiation in 3T3L1 cells.

TRA2B Splice Factor Expression in 3T3L1 Cells—Our previous study indicated that the expression patterns of the two alternatively spliced variants of PKCδ (PKCδI (via utilization of 5′ splice site I on exon 9) and PKCδII (via utilization of 5′ splice site II on exon 9)) are distinct in 3T3L1 cells. Alternative splicing is regulated by the interaction of trans-factors with the cis-elements on the pre-mRNA. To identify the splice factor involved in PKCδI splicing during early differentiation stage in preadipocytes, we used 16H3 antibody (Millipore). This widely used antibody by RNA biologists detects multiple SR proteins ranging from 20 to 75 kDa. Our results showed a protein at ~35 kDa whose pattern corresponded to the expression of PKCδI, *i.e.* high expression on day 0 and then tapering down during the following days. Using specific antibodies, our results indicated that SFRS10 (also known as TRA2B/Tra2β) expression was high on day 0 followed by a gradual decline (Fig. 4*a*). SRSF1 (also known as SF2/ASF) and SRSF2 (also known as SC35), whose molecular mass, is also around ~35 kDa were also individually analyzed for their expression patterns in 3T3L1 cells, and data showed that the PKCδI levels expression did not concur with their expression patterns (data not shown). These results indicated that Tra2β expression was concurrent with PKCδI expression in 3T3L1 cells. Using computational analysis, we determined that the consensus binding sequence of Tra2β (17) was present on PKCδI exon 9 (Fig. 4*b*).

Tra2β Mediates PKCδI Splicing—Because our results above indicated a potential role of TRA2B in PKCδI splicing, we sought to evaluate this further. We transfected TRA2B siRNA (Origene; 10 nM) on day −1 along with its scrambled control, and harvested the cells on day 2 of 3T3L1 *in vitro* differentiation. Our results (Fig. 5*a*) show a decrease of PKCδI levels with TRA2B siRNA, whereas PKCδII levels remain unchanged. We confirmed the results with SYBR Green qPCR (Fig. 5*b*). Next, we overexpressed TRA2B (2 μg) on day 6 when both PKCδI and TRA2B levels are lower in differentiating 3T3L1 cells and analyzed cells on day 8. Our results (Fig. 5*c*) indicated an increase in PKCδI levels with overexpression of TRA2B. These results demonstrate that TRA2B mediated PKCδI splicing.

Inclusion of PKCδI Exon in a Splicing Minigene—Splicing minigenes are advantageous to study alternative splicing events without the influence of endogenous factors. Hence to evaluate the role of TRA2B in PKCδI alternative splicing, we cloned heterologous splicing minigenes which contained PKCδI exon 9 and its flanking 3′ and 5′ sequences cloned into a splicing vector pSPL3 (see "Experimental Procedures"). The splicing minigene A contained the alternative 5′ splice site II, whereas splicing minigene B was trimmed to contain minimum 5′ flanking sequences without additional 5′ splice sites. Splicing minigenes A or B or pSPL3 vector was transiently transfected on day 0. 3T3L1 cells were differentiated for 48 h. RNA was isolated and RT-PCR performed using primers for SD (splice donor exon of pSPL3) and SA (splice acceptor exon of pSPL3). Our results show (Fig. 6) PKCδI exon inclusion via utilization of 5′ splice site I in the splicing minigenes A and B in 3T3L1 cells. The 5′ splice site II was not utilized at this stage of differentiation in 3T3 preadipocytes.

Mutation of PKCδ Splicing Minigene—Our computational analysis of PKCδ exon 9 showed the presence of a TRA2B consensus binding sequence gagaagaa. To determine whether Tra2β bound to the cis-element to promote PKCδI splicing, we mutated this TRA2B sequence within the PKCδ splicing minigene A (referred to as pSPL3-PKCδ**T2B splicing minigene; schematic in Fig. 7*a*). 3T3L1 cells were transfected on day 0 with either splicing minigene A or mutated pSPL3-PKCδ**T2B splicing minigene along with Tra2β (2 μg). Cells were then differentiated for 24 h. This enabled quantification of the response of Tra2β on PKCδ exon 9 inclusion as 48 h differentiation in Fig. 6 resulted in maximum PKCδI inclusion. RNA was collected, and PKCδI exon inclusion was evaluated by PCR using SD-SA primers. Our results (Fig. 7*b*) indicated that Tra2β increased PKCδI exon 9 inclusion using 5′ splice site I in the splicing minigene A and that mutation of TRA2B sequence inhibited inclusion of PKCδI exon9. This demonstrates that TRA2B mediated splicing of PKCδI mRNA.

Tra2β Binds to PKCδI Pre-mRNA—To establish that Tra2β bound to PKCδ mRNA, we performed RIP. The RIP assay involves immunoprecipitation of complexes formed endogenously between the RNA-binding proteins along with the associated RNA *in vivo*. 3T3L1 cells were collected on day 0 when they were 100% confluent. The complex was cross-linked *in vivo* using formaldehyde. Tra2β antibody was used to immunoprecipitate the complex. A negative control (mock IgG IP) or positive control (SNRNP70 IP) for RIP assay was included in the experiments. Supernatant (50 μl) after the last wash was ali-

FIGURE 3. **3T3L1 preadipocytes were transfected with PRKCD siRNA or scrambled siRNA and maintained in culture through differentiation for 3 days.** *a*, Oil Red O staining for lipid accumulation. *b*, quantification of absorbance of Oil Red O assay. Statistical analysis was performed by two-tail Student's *t* test; *** $p < 0.0001$ highly significant between day 3 scrambled siRNA control and PRKCD siRNA. *c*, whole cell lysates were harvested on day 3 and immunoblotted (*IB*) with anti-PPARγ, anti-adiponectin, anti-PKCδ (which can detect PKCδI and PKCδII), PKCδII-specific antibody separately as its expression levels are very low, or anti-β-actin as indicated. PKCδI levels were reduced by 80%. Experiments were repeated five times with similar results. The graph represents densitometric units normalized to β-actin. *d*, in separate experiments, PRKCD siRNA, PKCδII-specific siRNA, or scrambled control was transfected and maintained in culture. Cells were harvested on day 3. SYBR Green real time qPCR was performed for PPARγ1 and -γ2, adiponectin, PKCδI, and PKCδII. *RQ*, relative quantification. Experiments were repeated five times. Statistical analysis was performed by two-tail Student's *t* tests; ***, $p < 0.0001$ highly significant on day 3 between scrambled siRNA control and PRKCD siRNA for PPARγ1, PPARγ2, and adiponectin.

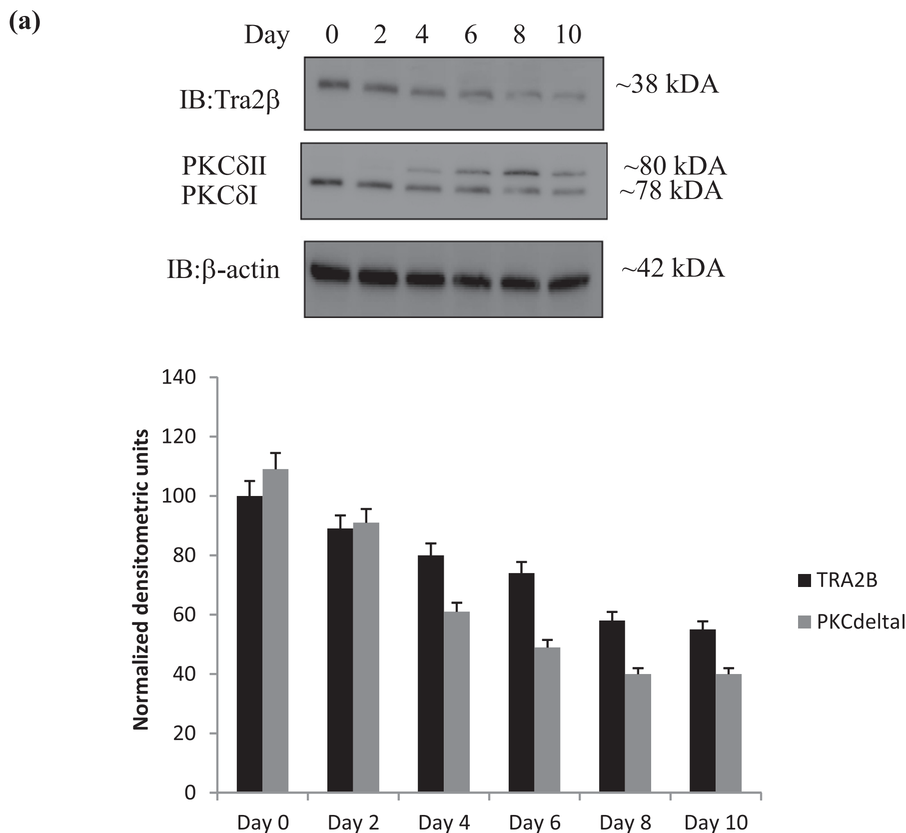

(b) Tra2β sequence on PKCδI Exon 9

taccagggat ttg**agaagaa** gccagaagtc tctgggagtg acatcctagg tgaagctggg

FIGURE 4. *a*, 3T3L1 preadipocytes were differentiated *in vitro*, and whole cell lysates were collected every 2 days from day 0 to day 10. Western blot (*IB*) analysis was performed using Tra2β antibody, PKCδ antibody (which can detect PKCδI and PKCδII simultaneously), or β-actin. The graph shows quantification of normalized densitometric units. The experiment was independently repeated five times with similar results. *b*, Tra2β sequence on PKCδI exon 9 and schematic of its position (*E* = exon on the schematic).

quoted for use in a Western blot to confirm IP. The cross-linking was reversed and extracted RNA from the RIP was then used in qPCR. For positive control, qPCR was performed using U1 RNA primers, the binding partner for SNRNP70. Our results (Fig. 8) showed enrichment of PKCδI with Tra2β RIP.

DISCUSSION

PKCδ has roles in cellular differentiation, proliferation, and apoptosis. The role of PKCδI splice variant in apoptosis was previously shown by us (9) and others (18, 19). Here we evaluated the role of PKCδI during early stages (0–48 h) of 3T3L1 differentiation. PKCδI is the predominant splice variant present in 3T3L1 preadipocytes; PKCδII is not expressed significantly in the early stages of differentiation. Studies have pointed to the role of PKCδ in cell cycle. In adipocytes, these were limited to day 0 compared with day 8 (20). To our knowledge no study was undertaken to delineate the roles and mechanism of expression of PKCδI splice variant during early stages of 3T3L1 differentiation. PKCδ can be both stimulatory and inhibitory in the cell cycle. PKC effects on cell cycle are generally mediated by downstream signaling cascades such as PI3K/Akt, Erk, or Wnt pathway. PKCδ affects activity of cyclin-dependent kinases as well as cyclin D1, cyclin E, or cyclin A and promotes phosphorylation of the retinoblastoma (Rb) protein (21, 22). It was shown that PKCδ stimulated G_1 phase cell cycle progression in rat Wistar thyroid cells (23) and that PKCδ inhibits G_1 cell cycle progression in response to testosterone in coronary smooth muscle cells (24). Phorbol 12-myristate 13-acetate-induced degradation of PKCδ requires its phosphorylation in NIH3T3 cells (25). PKCδ is required to maintain G_2/M checkpoint in keratinocytes in response to UV radiation (26). Here we showed that down-regulation of PKCδI during 3T3L1 adipogenesis was required for differentiation to adipocytes. The 3T3L1 cells undergo mitotic clonal expansion, which is supported by high levels of PKCδI and exit from the cell cycle to initiate differentiation is regulated by PKCδI. Further in-depth

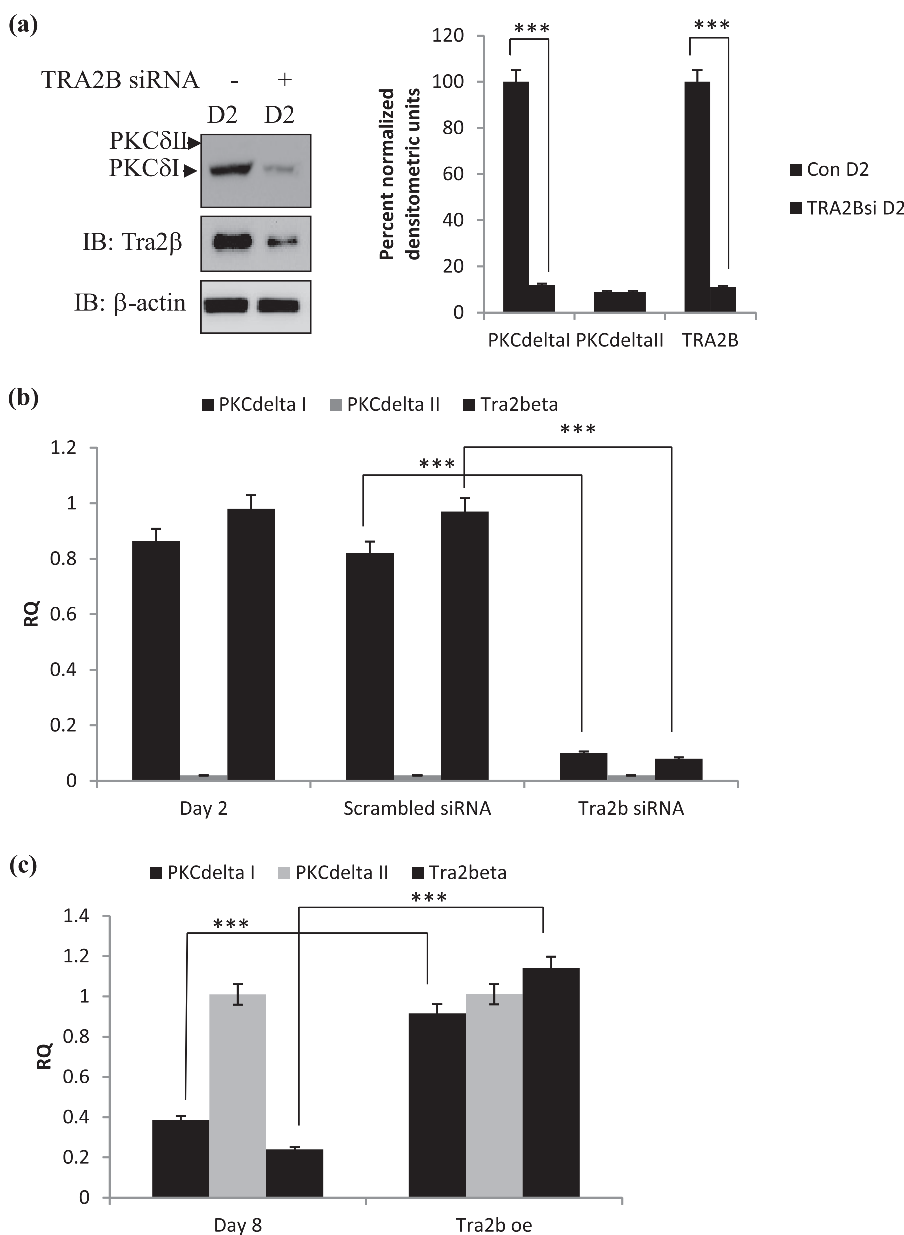

FIGURE 5. *a*, 3T3L1 preadipocytes were transfected with TRA2B siRNA on day 0 and maintained in culture through differentiation for 2 days. Western blot (*IB*) analysis was performed with PKCδ antibody or Tra2β antibody. Experiments were repeated four times with similar results. The graph shows quantification of normalized units. *b*, 3T3L1 preadipocytes were transfected with TRA2B siRNA or scrambled siRNA on day 0 and maintained in culture through differentiation for 2 days. SYBR Green real time qPCR was performed using primers for PKCδI, PKCδII, or TRA2B using GAPDH as the internal control. The experiment was independently repeated four times with similar results. Statistical analysis performed by two-tail Student's *t* test; ***, $p < 0.0001$ highly significant between control day2 and TRA2B siRNA day 2 for PKCδI. *RQ*, relative quantification. *c*, Tra2β (2 μg) was transiently transfected on day 6, and whole cell lysates were collected on day 8. SYBR Green real time qPCR was performed using primers for TRA2B, PKCδI, or PKCδII. The experiment was independently repeated four times with similar results. Statistical analysis performed by two-tail Student's *t* test; ***, $p < 0.0001$ highly significant between control day 8 and TRA2B overexpression day 8 for PKCδI.

analysis would be required to identify the specific cyclin or cyclin-dependent kinases and their phosphorylation cascades as well as cross-talk that mediates this effect of PKCδI in 3T3L1 cells.

Alternative splicing of PRKCD gene produces the splice variants PKCδI and PKCδII in 3T3L1 cells. During adipogenesis, the expression pattern of these PKCδ splice variants is distinct. PKCδI is present in preadipocytes, and its expression slowly declines after differentiation, whereas PKCδII expression increases after terminal differentiation. Alternative splicing is an essential mode for protein diversity and gives the ability to adjust to the constantly changing proteomic needs of the cell in response to development, hormones, and other stimuli. These changes are often a result of the dynamic association of the splice factors with pre-mRNA of the target gene. Pre-mRNA splicing is catalyzed by the spliceosome, which has >200 components including small nuclear ribonucleoproteins and proteins. Protein factors that function as enhancers and suppressors of splicing are an integral part of the spliceosome (27). In 3T3L1 cells, TRA2B mediates the splicing of PKCδI mRNA by binding to its cis-element on PKCδI exon 9. This site is close to the 5′ splice site, and binding of Tra2β promotes the binding of

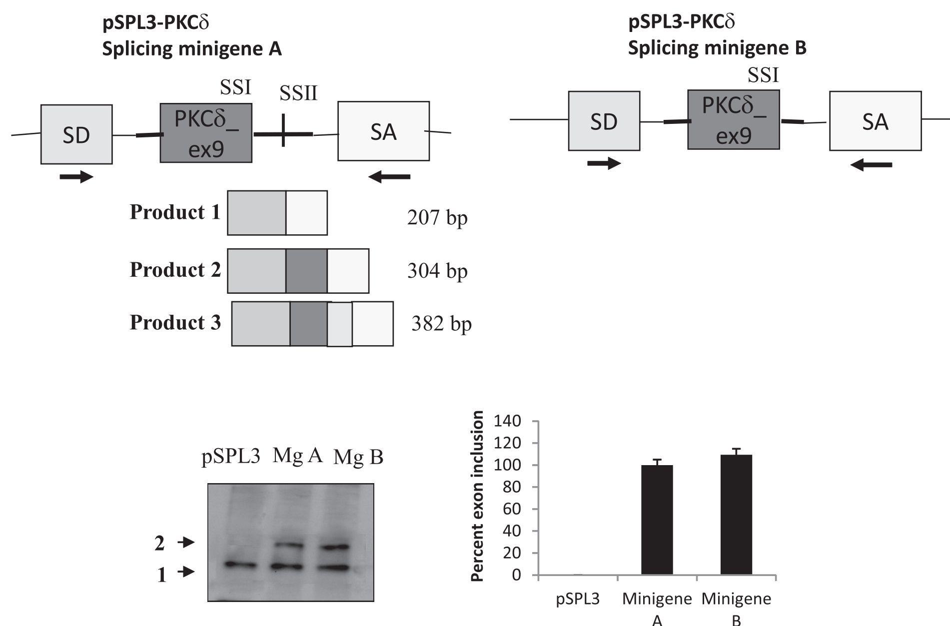

FIGURE 6. **Schematic of PKCδ exon 9 and its 3′ and 5′ flanking introns cloned into the splicing vector pSPL3.** Splicing minigene A (*Mg A*)contains the alternate 5′ splice site, whereas splicing minigene B (*Mg B*) is deleted to exclude the alternate 5′ splice site (*bold lines* flanking PKCδ exon 9 depict the size of the insert). *Arrows* indicate SD (splice donor exon) and SA (splice acceptor exon) primer positions. Schematic of expected PCR products and their sizes are shown: *1*, constitutive splicing of SD to SA; *2*, inclusion of PKCδ exon9 using 5′ splice site I; *3*, product utilizing 5′ splice site II. The pSPL3 splicing vector or the splicing minigenes were transfected in differentiating adipocytes (day 0), and RNA was harvested on day 2. PCR performed using SD-SA primers. Products were separated by PAGE and were silver-stained for visualization. 5′ splice site II was not utilized on day 2 in the splicing minigene assay; constitutive splicing of SD to SA serves as a positive control for the assay. Graphs represent the percent exon inclusion calculated as SS I/(SS I + SSII) × 100 in the samples and are representative of five experiments performed separately.

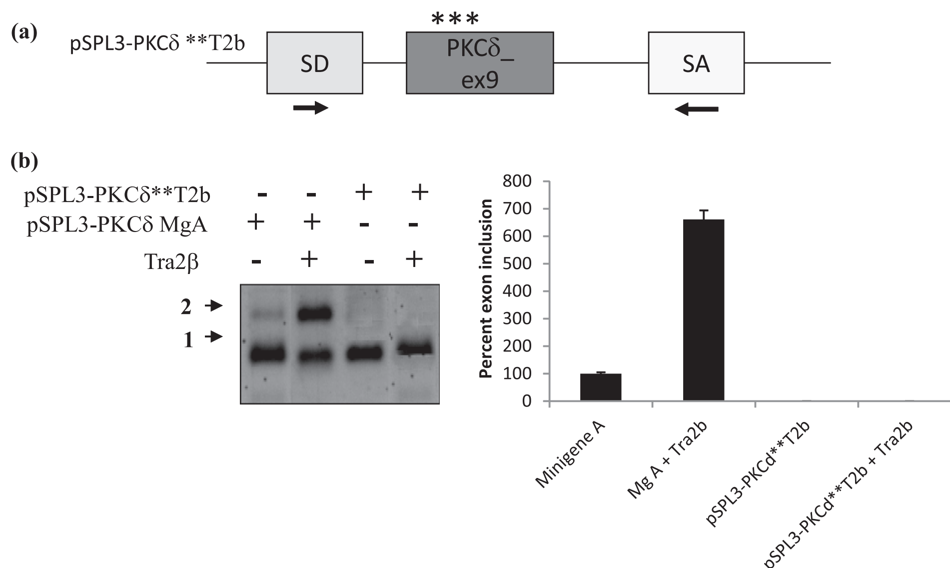

FIGURE 7. **Mutation of Tra2β site on PKCδ splicing minigene.** *a*, schematic of Tra2β binding site mutated within pSPL3-PKCδ splicing minigene. *** on the schematic indicates mutated Tra2β binding site. *Arrows* indicate primer positions on splice donor exon (*SD*) and splice acceptor exon (*SA*). *b*, either splicing minigene A (*Mg A*) or pSPL3-PKCδ**T2b splicing minigene was co-transfected along with 2 μg of Tra2β in differentiating adipocytes (day 0), and RNA was harvested 24 h later on day 1. PCR was performed using SD-SA primers. Products were separated by PAGE and were silver-stained for visualization. Product 1 is SD-SA constitutive splicing; product 2 is PKCδ exon inclusion using 5′ splice site I (*SSI*). Graphs represent percent exon inclusion calculated as SS I/(SS I + SSII) × 100 in the samples and are representative of four experiments performed separately. The experiment was independently repeated five times with similar results.

U1 small nuclear ribonucleoprotein to the 5′ splice site thereby initiating the splicing reaction. Because several endogenous factors could potentially affect PKCδI splicing, we also used a heterologous splicing minigene to validate the role of TRA2B in promoting PKCδI splicing during 3T3L1 adipogenesis. The 5′ splice site II was not utilized upon TRA2B mutation in the minigene, which suggests that utilization of the downstream splice site required splice factors that may be absent during 0–24 h of differentiation of 3T3L1 preadipocytes. Our studies point to the role of TRA2B in cell cycle progression. It is possible that TRA2B affects splicing of other genes involved in the cell cycle; however, this remains to be elucidated.

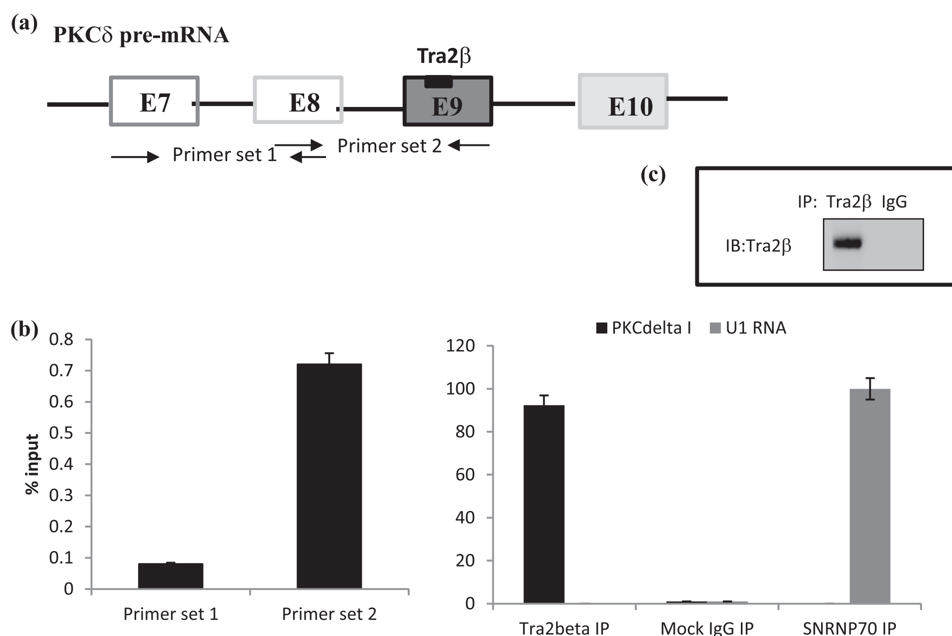

FIGURE 8. **RIP assay was performed on 3T3L1 on day 1 of differentiation.** Immunoprecipitated RNA was analyzed by two primer sets for PKCδ as shown on the schematic. *a*, primer set 1 amplifies the region downstream of PKCδI exon 9, whereas primer set 2 amplifies PKCδI exon 9 containing the TRA2B binding site. Graphs are plotted as the percentage of total input before immunoprecipitation using primer sets 1 and 2 (*b*) and -fold enrichment of PKCδI using qPCR in the RIP assay with Tra2*β* IP (*c*); -fold enrichment of U1 RNA using SNRP70 IP (positive control). Results show Tra2*β* binding on PKCδI exon 9. The *inset* shows immunoblot (*IB*) of Tra2*β* IP and IgG IP (negative control) using antibody against Tra2*β*. Experiments were repeated four times with similar results.

Regulation of alternative splicing by TRA2B is shown in several systems including LIPN1 in liver (28), splicing of myosin phosphatase targeting subunit 1 in smooth muscle (29), splicing of Tau in neurons (30) and BRCA1 gene (31). TRA2B is also shown to be involved in mouse embryogenesis and spermatogenesis as well as in meiosis in male germ cells (32). Our previous study demonstrated dysregulated PKCδ alternative splicing in obese adipocytes (1) compared with lean. Furthermore, the adipogenesis program was also dysregulated in obese subjects. Hence, understanding the regulation of expression of PKCδI by splice factor TRA2B during adipogenesis is important to the study of obesity pathology.

Acknowledgment—We thank Andre Apostolatos for technical assistance in laboratory.

REFERENCES

1. Carter, G., Apostolatos, A., Patel, R., Mathur, A., Cooper, D., Murr, M., and Patel, N. A. (2013) Dysregulated alternative splicing pattern of PKC during differentiation of human preadipocytes represents distinct differences between lean and obese adipocytes. *ISRN Obes.* **2013,** 161345
2. Patel, R., Apostolatos, A., Carter, G., Ajmo, J., Gali, M., Cooper, D. R., You, M., Bisht, K. S., and Patel, N. A. (2013) Protein kinase Cδ (PKCδ) splice variants modulate apoptosis pathway in 3T3L1 cells during adipogenesis: identification of PKCδII inhibitor, *J. Biol. Chem.* **288,** 26834–26846
3. Green, H., and Kehinde, O. (1979) Formation of normally differentiated subcutaneous fat pads by an established preadipose cell line. *J. Cell. Physiol.* **101,** 169–171
4. Green, H., and Kehinde, O. (1975) An established preadipose cell line and its differentiation in culture. II. Factors affecting the adipose conversion. *Cell* **5,** 19–27
5. Brun, R. P., and Spiegelman, B. M. (1997) PPARγ and the molecular control of adipogenesis. *J. Endocrinol.* **155,** 217–218
6. Farmer, S. R. (2005) Regulation of PPARγ activity during adipogenesis. *Int. J. Obes.* **29,** S13–S16
7. Rosen, E. D., and MacDougald, O. A. (2006) Adipocyte differentiation from the inside out. *Nat. Rev. Mol. Cell Biol.* **7,** 885–896
8. Nishizuka, Y. (1986) Studies and prespectives of protein kinase C. *Science* **233,** 305–312
9. Patel, N. A., Song, S. S., and Cooper, D. R. (2006) PKCδ alternatively spliced isoforms modulate cellular apoptosis in retinoic acid-induced differentiation of human NT2 cells and mouse embryonic stem cells. *Gene Exp.* **13,** 73–84
10. Apostolatos, H., Apostolatos, A., Vickers, T., Watson, J. E., Song, S., Vale, F., Cooper, D. R., Sanchez-Ramos, J., and Patel, N. A. (2010) Vitamin A metabolite, all-trans-retinoic acid, mediates alternative splicing of protein kinase C δVIII (PKCδVIII) isoform via splicing factor SC35. *J. Biol. Chem.* **285,** 25987–25995
11. Beil, B., Screaton, G., and Stamm, S. (1997) Molecular cloning of htra2-*β*-1 and htra2-*β*-2, two human homologs of tra-2 generated by alternative splicing. *DNA Cell Biol.* **16,** 679–690
12. Manley, J. L., and Krainer, A. R. (2010) A rational nomenclature for serine/arginine-rich protein splicing factors (SR proteins). *Genes Dev.* **24,** 1073–1074
13. Dauwalder, B., Amaya-Manzanares, F., and Mattox, W. (1996) A human homologue of the *Drosophila* sex determination factor transformer-2 has conserved splicing regulatory functions. *Proc. Natl. Acad. Sci. U.S.A.* **93,** 9004–9009
14. Hofmann, Y., Lorson, C. L., Stamm, S., Androphy, E. J., and Wirth, B. (2000) Htra2-*β* 1 stimulates an exonic splicing enhancer and can restore full-length SMN expression to survival motor neuron 2 (SMN2). *Proc. Natl. Acad. Sci. U.S.A.* **97,** 9618–9623
15. Stoilov, P., Daoud, R., Nayler, O., and Stamm, S. (2004) Human tra2-*β*1 autoregulates its protein concentration by influencing alternative splicing of its pre-mRNA, *Hum. Mol. Genet.* **13,** 509–524
16. Apostolatos, A., Song, S., Acosta, S., Peart, M., Watson, J. E., Bickford, P., Cooper, D. R., and Patel, N. A. (2012) Insulin promotes neuronal survival via the alternatively spliced protein kinase CδII isoform. *J. Biol. Chem.* **287,** 9299–9310
17. Elliott, D. J., Best, A., Dalgliesh, C., Ehrmann, I., and Grellscheid, S. (2012) How does Tra2*β* protein regulate tissue-specific RNA splicing? *Biochem. Soc. Trans.* **40,** 784–788
18. Carvour, M., Song, C., Kaul, S., Anantharam, V., Kanthasamy, A., and

Kanthasamy, A. (2008) Chronic low-dose oxidative stress induces caspase-3-dependent PKCδ proteolytic activation and apoptosis in a cell culture model of dopaminergic neurodegeneration. *Ann. N.Y. Acad. Sci.* **1139,** 197–205

19. Kanthasamy, A. G., Kitazawa, M., Yang, Y., Anantharam, V., and Kanthasamy, A. (2008) Environmental neurotoxin dieldrin induces apoptosis via caspase-3-dependent proteolytic activation of protein kinase Cδ (PKCδ): implications for neurodegeneration in Parkinson's disease. *Mol. Brain* **1,** 12
20. Zhou, Y., Wang, D., Li, F., Shi, J., and Song, J. (2006) Different roles of protein kinase C-βI and -δ in the regulation of adipocyte differentiation. *Int. J. Biochem. Cell Biol.* **38,** 2151–2163
21. Fukumoto, S., Nishizawa, Y., Hosoi, M., Koyama, H., Yamakawa, K., Ohno, S., and Morii, H. (1997) Protein kinase Cδ inhibits the proliferation of vascular smooth muscle cells by suppressing G_1 cyclin expression. *J. Biol. Chem.* **272,** 13816–13822
22. Grossoni, V. C., Falbo, K. B., Kazanietz, M. G., de Kier Joffé, E. D., and Urtreger, A. J. (2007) Protein kinase Cδ enhances proliferation and survival of murine mammary cells. *Mol. Carcinog.* **46,** 381–390
23. Santiago-Walker, A. E., Fikaris, A. J., Kao, G. D., Brown, E. J., Kazanietz, M. G., and Meinkoth, J. L. (2005) Protein kinase Cδ stimulates apoptosis by initiating G_1 phase cell cycle progression and S phase arrest. *J. Biol. Chem.* **280,** 32107–32114
24. Bowles, D. K., Maddali, K. K., Dhulipala, V. C., and Korzick, D. H. (2007) PKCδ mediates anti-proliferative, pro-apoptic effects of testosterone on coronary smooth muscle. *Am. J. Physiol. Cell Physiol.* **293,** C805–C813
25. Srivastava, J., Procyk, K. J., Iturrioz, X., and Parker, P. J. (2002) Phosphorylation is required for PMA- and cell-cycle-induced degradation of protein kinase Cδ. *Biochem. J.* **368,** 349–355
26. LaGory, E. L., Sitailo, L. A., and Denning, M. F. (2010) The protein kinase Cδ catalytic fragment is critical for maintenance of the G_2/M DNA damage checkpoint. *J. Biol. Chem.* **285,** 1879–1887
27. Bourgeois, C. F., Lejeune, F., and Stévenin, J. (2004) Broad specificity of SR (serine/arginine) proteins in the regulation of alternative splicing of pre-messenger RNA. *Prog. Nucleic Acid Res. Mol. Biol.* **78,** 37–88
28. Pihlajamäki, J., Lerin, C., Itkonen, P., Boes, T., Floss, T., Schroeder, J., Dearie, F., Crunkhorn, S., Burak, F., Jimenez-Chillaron, J. C., Kuulasmaa, T., Miettinen, P., Park, P. J., Nasser, I., Zhao, Z., Zhang, Z., Xu, Y., Wurst, W., Ren, H., Morris, A. J., Stamm, S., Goldfine, A. B., Laakso, M., and Patti, M. E. (2011) Expression of the splicing factor gene SFRS10 is reduced in human obesity and contributes to enhanced lipogenesis. *Cell Metab.* **14,** 208–218
29. Fu, K., Mende, Y., Bhetwal, B. P., Baker, S., Perrino, B. A., Wirth, B., and Fisher, S. A. (2012) Tra2β protein is required for tissue-specific splicing of a smooth muscle myosin phosphatase targeting subunit alternative exon. *J. Biol. Chem.* **287,** 16575–16585
30. Glatz, D. C., Rujescu, D., Tang, Y., Berendt, F. J., Hartmann, A. M., Faltraco, F., Rosenberg, C., Hulette, C., Jellinger, K., Hampel, H., Riederer, P., Möller, H. J., Andreadis, A., Henkel, K., and Stamm, S. (2006) The alternative splicing of tau exon 10 and its regulatory proteins CLK2 and TRA2-β1 changes in sporadic Alzheimer's disease. *J. Neurochem.* **96,** 635–644
31. Raponi, M., Smith, L. D., Silipo, M., Stuani, C., Buratti, E., and Baralle, D. (2014) BRCA1 exon 11 a model of long exon splicing regulation. *RNA Biol.* **11,** 351–359
32. Grellscheid, S., Dalgliesh, C., Storbeck, M., Best, A., Liu, Y., Jakubik, M., Mende, Y., Ehrmann, I., Curk, T., Rossbach, K., Bourgeois, C. F., Stévenin, J., Grellscheid, D., Jackson, M. S., Wirth, B., and Elliott, D. J. (2011) Identification of evolutionarily conserved exons as regulated targets for the splicing activator tra2β in development. *PLoS Genet.* **7,** e1002390